Title

Isolation of psychedelic-responsive neurons underlying anxiolytic behavioral states

Journal

Science, 386(6723)

ISSN

0036-8075

Authors

Muir, J

Lin, S

Aarrestad, IK

et al.

Publication Date

2024-11-15

DOI

10.1126/science.adl0666

Peer reviewed

HHS Public Access

Author manuscript

Science. Author manuscript; available in PMC 2024 November 25.

Published in final edited form as:

Science. 2024 November 15; 386(6723): 802–810. doi:10.1126/science.adl0666.

Isolation of psychedelic-responsive neurons underlying anxiolytic behavioral states

J. Muir[1,2,†], **S. Lin**[1,2,†], **I. K. Aarrestad**[3,4], **H. R. Daniels**[1,2], **J. Ma**[1,2], **L. Tian**[1,5,‡], **D. E. Olson**[1,4,5,6], **C. K. Kim**[1,2,4,*]

[1]Center for Neuroscience, University of California, Davis, Davis, CA 95618, USA.

[2]Department of Neurology, School of Medicine, University of California, Davis, Sacramento, CA 95817, USA.

[3]Neuroscience Graduate Group, University of California, Davis, Davis, CA 95616, USA.

[4]Institute for Psychedelics and Neurotherapeutics, University of California, Davis, Davis, CA 95616, USA.

[5]Department of Biochemistry and Molecular Medicine, School of Medicine, University of California, Davis, Sacramento, CA 95817, USA.

[6]Department of Chemistry, University of California, Davis, Davis, CA 95616, USA.

Abstract

Psychedelics hold promise as alternate treatments for neuropsychiatric disorders. However, the neural mechanisms by which they drive adaptive behavioral effects remain unclear. We isolated the specific neurons modulated by a psychedelic to determine their role in driving behavior. Using a light- and calcium-dependent activity integrator, we genetically tagged psychedelic-responsive neurons in the medial prefrontal cortex (mPFC) of mice. Single-nucleus RNA sequencing revealed that the psychedelic drove network-level activation of multiple celltypes beyond just those expressing 5-hydroxytryptamine 2A receptors. We labeled psychedelic-responsive mPFC neurons with an excitatory channelrhodopsin to enable their targeted manipulation. We found that reactivation of these cells recapitulated the anxiolytic effects of the psychedelic without driving

*Corresponding author. ckk@princeton.edu.
†These authors contributed equally to this work.
‡Present address: Max Planck Florida Institute for Neuroscience, Jupiter, FL 33458, USA.

Author contributions: CKK, JM and SL designed all experiments. SL initiated the study and performed initial pilot experiments. SL and JM performed mouse stereotaxic surgeries, behavior experiments, and behavior data analysis. JM performed GRIN lens imaging and 2-photon imaging data analysis. JM performed snRNA-seq experiments and data analysis. IKA, HRD and JMa performed scoring of head twitch behavior. DEO provided guidance on the use of DOI and interpretation of behavioral experiments. LT provided the psychLight2 virus and guidance on data interpretation. JM, SL, and CKK wrote, reviewed, and edited the paper, with comments from all authors. CKK supervised all aspects of the project.

Competing interests: DEO is a co-founder of Delix Therapeutics, Inc. and serves as the chief innovation officer and head of the scientific advisory board. All other authors declare no other competing interests.

Supplementary Materials
Materials and Methods
Figs. S1 to S10
Table S1
References (46–50)
Data S1 to S4

its hallucinogenic-like effects. These findings reveal essential insight into the cell-type-specific mechanisms underlying psychedelic-induced behavioral states.

Neuropsychiatric illnesses are among the leading causes of disability worldwide (1), yet treatments for these disorders remain effective in only 50% of the population (2), reflecting a serious need for more diverse treatments. Recently, psychedelics have reemerged as potential therapeutics for treating several neuropsychiatric conditions (3). Classic psychedelics act on serotonergic 5-hydroxytryptamine type 2A receptors (5-HT2ARs) (4) by promoting dendritic spine formation, increasing plasticity, and inducing transcriptional changes in neurons (5–10). At the behavioral level in animals, psychedelics have been shown to induce adaptations such as reduced passive coping, improved fear extinction, and reduced anxiety-like behavior (10–16), in addition to the characteristic acute hallucinogenic-like effects of these drugs (17–19). The advent of nonhallucinogenic analogues of psychedelics with therapeutic properties has suggested that distinct neural circuits may mediate the therapeutic and hallucinogenic properties of psychedelics (20–22), but these putative circuit mechanisms have yet to be defined. We posited that psychedelics target a functionally distinct population of neurons in the medial prefrontal cortex (mPFC), driving network-level activity that ultimately leads to their beneficial effects.

Targeting functionally relevant populations of neurons activated by psychedelics has been challenging due to a lack of suitable molecular toolboxes. However, a new class of molecular technologies called neural activity integrators (23, 24) now allows for genetic tagging of neurons specifically activated during an acute experimental time window (1 to 15 minutes), such as during the administration of a drug. Here, we used a light- and calcium-dependent activity integrator, scFLARE2 (24), to tag, molecularly profile, and manipulate mPFC neurons activated by a psychedelic, 2,5-dimethoxy-4-iodoamphetamine (DOI). We isolated a psychedelic-responsive network that extends beyond the direct target of 5-HT2AR-expressing neurons and recapitulates the anxiolytic, but not the hallucinogenic, properties of these drugs.

The anxiolytic properties of DOI outlast 5-HT2AR binding and its hallucinogenic effects.

Previous studies have shown that 5-HT2AR activation not only mediates the hallucinogenic properties of psychedelics, but also contributes to their beneficial effects on depressive and anxiety-like behaviors (10, 11, 14, 19, 25). One of the most well-characterized serotonergic psychedelics, DOI, reduces anxiety-like behavior during the marble-burying test (MBT) and the elevated plus maze (EPM) in a 5-HT2AR-dependent manner (26, 27). DOI also reliably elicits a head twitch response (HTR) in rodents, which is used to model the hallucinogenic properties of psychedelics and is tightly coupled to 5-HT2AR activation (18, 28). However, it is unknown whether these anxiolytic effects outlast the immediate 5-HT2AR activation and behavioral disruptions caused by psychedelic action.

To compare the behavioral effects of psychedelics during and after 5-HT2AR activation, we first determined the time course of DOI presence in the brain using a 5-HT2AR-based

fluorescent biosensor, psychLight2 (29). Given that the binding pockets of pyschLight2 and native 5-HT2ARs are identical (29), the inhibition constant (K_i) values for serotonergic ligands at these receptors are equivalent (30), and activation of psychLight2 by psychedelics correlates exceptionally well with BRET-based measures of 5-HT2AR activation (30), psychLight activity should faithfully report the timescale of DOI presence in vivo in the mPFC. We injected male and female mice with psychLight2 adeno-associated viruses (AAVs) in the mPFC and implanted a fiber optic cannula to measure fluorescence in vivo (Fig. 1A, and fig. S1A). After injection with DOI, the fluorescence signal peaked within 30 minutes and slowly decayed over the course of 4 hours (Fig. 1B and fig. S1B). Analysis of the mean fluorescence over 30-minute time bins revealed that after 3.5 hours, there was no observable psychLight2 signal above baseline (Fig. 1C). This decay was not due to fluorescent protein depletion after 4 hours of recording, because a delayed DOI injection after 3 hours still drove a robust increase in fluorescence (fig. S1C). These data show that 4 hours after DOI injection, the psychLight2 signal and the presence of DOI are greatly diminished. Our data closely match prior literature showing that the half-life of DOI measured in the blood and from the forebrain of mice is ~2 hours (28).

We then confirmed that both male and female mice exhibit reductions in marble burying when assayed 30 minutes after an injection of DOI (near the peak of psychLight2 activity), compared with control mice injected with saline (Fig. 1D,E, and fig. S2A). Mice treated with DOI exhibited a mild reduction in velocity compared with saline-treated mice, but still fully explored the marble arena during the task (fig. S2B). Because elevations in marble burying can also be a sign of compulsivity rather than anxiety-like behavior, we also performed the EPM, a standard test for anxiety-like behavior. Again, we observed that DOI induced an acute anxiolytic effect, with DOI-treated mice spending more time in the open arms compared with saline-treated mice (fig. S3A–E).

Consistent with previous literature, mice also showed an elevated HTR 30 minutes after DOI injection during the MBT (Fig. 1F, and fig. S2C). Linear discriminant analysis using either the number of marbles buried, or the number of HTRs could accurately predict whether mice were injected with saline or DOI at this time point (Fig. 1G).

Next, we measured behavior 6 hours after DOI injection, an additional 2.5 hours after the timepoint at which psychLight2 no longer detects the presence of DOI in the mPFC. We found that mice still exhibited a reduction in marble burying, indicating reduced anxiety-like behavior (Fig. 1H,I, and fig. S2D,E), but no longer exhibited elevated HTRs (Fig. 1J, and fig. S2F). The EPM performed at 6 hours also confirmed DOI's anxiolytic effect at this timepoint (fig. S3F–J). Linear discriminant analysis using the number of marbles buried could again accurately predict whether mice were injected with saline or DOI; however, classification using the number of HTRs performed poorly, near chance (Fig. 1K).

When mice injected with DOI were examined again 24 hours later, they unexpectedly buried more marbles compared with those injected with saline, possibly suggesting a psychedelic-induced, rebound anxiety-like phenotype (Fig. 1L,M). This rebound anxiety-like effect was more apparent in males than in females, and was also present at lower doses of DOI (fig.

S2G,H, and fig. S4). The EPM showed a trend for this anxiogenic effect at 24 hours, with more time spent in the closed arms of the maze (fig. S3K–O).

These data demonstrate that whereas both the anxiolytic- and hallucinogenic-like phenotypes are acutely induced by DOI administration, they may be partially dissociable, because only the anxiolytic effects appear to outlast the DOI presence in the mPFC. However, this anxiolytic effect does not persist to 24 hours (although we did not measure whether there were prolonged anxiolytic effects in the days after).

DOI drives elevated neuronal activity in a subset of mPFC neurons.

Given that prior studies in rodents have shown that direct stimulation of certain mPFC subpopulations drives anxiolytic-like effects (31), we posited that DOI may be increasing neuronal activity in a subset of neurons in the mPFC to mediate its anxiolytic properties. Although our psychLight2 experiments showed that DOI presence in the mPFC peaks at ~30 minutes and dissipates by 3.5 hours, this signal does not reflect the direct timescales of physiological cellular activity in response to DOI. This is because the psychLight2 is panneuronally expressed at higher amounts than the native 5-HT2AR, and only detects DOI binding to the engineered 5-HT2AR, rather than reporting downstream cellular activity or neuronal firing in the cells. Thus, to directly examine how DOI modulates neuronal activity in this region, we expressed the fluorescent calcium indicator GCaMP6f (32) in the mPFC and implanted a GRIN lens to enable single-cell 2-photon calcium imaging (Fig. 2A–D). We found that DOI immediately increased neuronal firing in ~54% of mPFC neurons, compared to 14% that were unaffected by DOI, and 32% that were inhibited by DOI (Fig. 2E,F). This is in contrast to prior reports finding that DOI primarily inhibits neuronal activity in most neurons in the rat frontal cortex regions (33, 34), and in the mouse visual cortex (35). These differences could reflect specific circuit properties of the mouse mPFC or differences in the recording modalities used to identify neurons (i.e., electrophysiology versus calcium imaging).

In a subset of mice, we also quantified the activity of the same mPFC neurons 30 minutes after the DOI injection, which is when we observed the maximal psychLight2 signal, and which also corresponds to when we performed our acute MBT and EPM assays. We found that DOI-activated neurons maintained their elevated activity at this 30-minute timepoint, but did not show signs of further increase (Fig. 2G, and fig. S5).

Genetically tagging a DOI-activated neural signature in the mPFC with scFLARE2.

We next wanted to examine the molecular and functional properties of these DOI-activated cells, so we investigated whether we could genetically tag DOI-activated cells using scFLARE2 (24), a recently described molecular activity integrator. This light- and calcium-gated transcription system records and then subsequently labels activated neurons with a reporter gene of choice (Fig. 2H). In response to coincident blue light and high intracellular calcium, scFLARE2 triggers the release of a non-native transcription factor (tTA), which drives the expression of a tTA-dependent tetracycline response element (TRE)-reporter gene.

The presence of this gene can be detected during single nucleus RNA sequencing (snRNA-seq) to determine activated cell-types, or it can encode an opsin to enable subsequent functional manipulation.

To validate scFLARE2 labeling, we injected mice with scFLARE2 and TRE::GFP reporter AAVs in the mPFC, and implanted a fiber optic cannula for blue light delivery. We then treated mice with either DOI or saline, and immediately delivered blue light stimulation for 15 minutes to drive scFLARE2 tagging of activated neurons. We chose this tagging window based on the timescale of activity observed with our 2-photon imaging results. Neurons exhibiting elevated activity during the 15-minute labeling window should get tagged with a green fluorescent protein (GFP) reporter gene. Mice were sacrificed 24 hours later for histological analysis (Fig. 2I). Image quantification showed that DOI-injected mice expressed more GFP+ cells compared with saline-injected control mice (Fig. 2J,K), with no differences in scFLARE2 viral expression (Fig. 2L). We found that on a cell-by-cell basis, ~40% of scFLARE2-expressing cells were activated (GFP+) in DOI-treated mice, as opposed to only 5% being activated in saline-treated mice (Fig. 2M). This percentage of activated cells was similar to that observed using 2-photon imaging. These results demonstrate that scFLARE2 can be used to label mPFC neurons activated by DOI.

Identification of cell-types activated by DOI using scFLARE2 and snRNA-seq.

We next investigated what transcriptional mPFC cell-types were being labeled by scFLARE2 during DOI activation using snRNA-seq. We injected mice in the mPFC with AAVs encoding scFLARE2 and a TRE-reporter gene transcript and implanted a fiber optic cannula for blue light delivery. After sufficient viral expression, mice were injected with either DOI or saline and given blue light stimulation for 15 minutes. After 24 hours, mice were sacrificed and their mPFC was microdissected and dissociated to generate a barcoded snRNA library for next-generation sequencing (Fig. 3A).

Dimensionality reduction and unsupervised clustering of the sequencing data identified the expected main cell-types present in the mPFC (fig. S6A). Neuronal cell-types were isolated and reclustered for further analysis. We identified nine different subclusters of neurons which could be distinguished on the basis of their expression of marker genes consistent with previous literature (36, 37): two subtypes of layer 2/3 excitatory neurons (L2/3–1 and L2/3–2), three subtypes of layer 5 excitatory neurons (L5–1 through L5–3), two subtypes of layer 6 neurons (L6–1 excitatory and L6–2 mixed), and two subtypes of inhibitory neurons (Sst/PV and Vip) (Fig. 3B,C). We could detect expression of the TRE-reporter gene and the scFLARE2 (tTA transcript) through sequencing across clusters (Fig. 3D,E, and fig. S6B).

Similar to the immunohistochemistry data shown in Fig. 2J–M, we confirmed that overall, neurons from DOI-injected mice had higher TRE-reporter gene expression than saline-injected mice (Fig. 3F), with no difference in tTA between groups (Fig. 3G, and fig. S6C). We then investigated whether the TRE-reporter gene was preferentially enriched in any of the clusters between DOI- versus saline-injected animals. We found an increase in both the mean expression of the TRE-reporter gene and in the fraction of TRE-reporter gene-positive

neurons in excitatory clusters L5–1 and L6–1, and in inhibitory cluster Sst/PV (Fig. 3H,I, and fig. S6D,E). These data suggest that DOI preferentially activates only a subset of neuronal subtypes in the mPFC.

Given that DOI targets the 5-HT2AR, which is a G_q coupled receptor, we investigated whether the TRE-reporter gene was enriched primarily in 5-HT2AR expressing neuron clusters (Htr2a+). We mapped the Htr2a transcript counts across neuronal clusters and identified those exhibiting enriched expression: L5–1, Sst/PV, and L6–2 (Fig. 4A–C). We then compared the Htr2a+ clusters with the DOI-activated clusters. DOI-activated clusters L5–1 and Sst/PV also exhibited enrichment in Htr2a, as expected. However, DOI-activated cluster L6–1 showed down-regulation of Htr2a expression. Moreover Htr2a+ cluster L6–2 was not among DOI-activated clusters. DOI is also known to agonize the 5-HT2C receptor, although its effects on marble burying do not appear to rely on activation of this receptor subtype (25), with mixed reports as to whether DOI's effects on HTR involve 5-HT2C receptors (38, 39). We found that the Htr2c transcript counts were upregulated in excitatory clusters L5–3 and L2/3–2 and inhibitory cluster Vip (Fig. 4D–F), none of which overlap with Htr2a-upregulated or DOI-activated clusters. These sequencing data thus suggest that DOI may be triggering network-level activation of neurons, extending beyond those thought to be directly modulated by psychedelics through 5-HT2AR (such as the L6–1 cluster).

Reactivation of DOI-tagged PFC neurons drives anxiolytic, but not hallucinogenic, behaviors.

After finding that DOI drives the excitation of specific subsets of mPFC neurons in vivo, we next investigated whether there was a causal relationship between the activity of these neurons and the anxiolytic behavioral phenotype that we identified previously. To test this idea, we envisioned tagging mPFC neurons activated by DOI with an excitatory opsin, and then re-activating them 24 hours later, when there was no longer an observable anxiolytic effect of the original DOI dose.

We injected mice in the mPFC with AAVs encoding scFLARE2 and TRE::mCherry-p2a-bReaChES, an excitatory red-shifted channelrhodopsin (40), and implanted a fiber-optic cannula for light delivery (fig. S7A). As before, we delivered blue light immediately after the injection. Thirty minutes after DOI injection, we performed a baseline MBT measurement, and 24 hours later, mice were reintroduced to the MBT along with orange light stimulation to reactivate tagged mPFC populations (Fig. 5A). Post-hoc histological analysis showed robust expression of TRE::mCherry-p2a-bReaChES reporter expression in the mPFC of scFLARE2-injected mice (Fig. 5B).

Control mice that received no orange light stimulation during the day 2 MBT exhibited similar marble burying behavior as wildtype un-infected mice in Fig. 1. DOI-injected mice showed reduced marble burying 30 minutes after treatment compared with saline-injected animals, an effect that did not persist to the following day (Fig. 5C, fig. S8A,B, and fig. S9A,B). However, mice that received orange light stimulation of DOI-activated neurons on day 2 showed reduced marble burying compared with mice receiving orange light stimulation of saline-activated neurons (Fig. 5D, and fig. S8C,D). Orange light stimulation

had no effect on locomotion in either group (fig. S9C,D). We also confirmed these findings using the EPM, showing that orange light stimulation of DOI-tagged neurons increased the amount of time that mice spent in the open arms of the EPM, indicating reduced anxiety (Fig. 5E,F, and fig. S10A–C).

To show the specificity of the DOI-activated neurons for reducing anxiety, we tested mice expressing a non-specific panneuronal mCherry-p2a-bReaChES virus in mPFC during the MBT 30 minutes and 24 hours after injection of DOI (Fig. 5G, fig. S7B). No differences in marble burying were observed on day 2 after injection in stimulated versus non-stimulated groups (Fig. 5H). These results indicate that stimulation of DOI-activated neurons in the mPFC 24 hours after treatment is sufficient to reproduce the acute anxiolytic effects of the drug.

Our snRNA-seq data showed that DOI activates both cell-types enriched in 5-HT2AR and those that are not. This led us to determine whether initial 5-HT2AR activation is necessary for scFLARE2 tagging of the DOI-activated mPFC neurons mediating the anxiolytic effects of the drug. We used a potent selective 5-HT2AR antagonist, volinanserin (M100907), which we showed blocks the acute anxiolytic effects of DOI on marble burying 30 minutes after injection (fig. S10D,E), as previously reported in the MBT (25) and EPM (41). In a separate cohort, mice underwent scFLARE2 labeling after injection with DOI or saline, in the presence of the antagonist (Fig. 5I). Orange light stimulation 24 hours after drug and antagonist injection had no effect on marble burying, indicating that the anxiolytic effects of DOI, and the tagging of a DOI-responsive anxiolytic network, rely on an initial 5-HT2AR activation (Fig. 5J).

Finally, given that we labeled mPFC neurons activated immediately after DOI injection, when mice exhibited both reduced anxiety and HTRs, we tested whether stimulation of these neurons elicited any hallucinogenic-like behaviors in mice. As before, DOI-injected mice displayed elevated HTRs compared with saline-injected mice on day 1; however, these same mice did not increase HTRs during orange light stimulation of DOI-activated neurons on day 2 (Fig. 5K, and fig. S8E,F).

Together these data demonstrate that reactivation of a DOI-responsive population in the mPFC is sufficient to drive the anxiolytic properties of a psychedelic, without reinstating its hallucinogenic effects.

Discussion

In some clinical trials, psychedelics have shown promise for improving the symptoms of anxiety and depression after even a single dose (42, 43). Understanding the mechanism of action of these drugs is essential for developing new treatments, especially for treatment-resistant populations. Here we investigated the mechanisms of psychedelic action in the mouse mPFC, finding that DOI drives activity in a functionally distinct network of neurons that are sufficient for recreating an anxiolytic behavioral state, independently of the hallucinogenic effects of these drugs.

Psychedelics are known to drive structural and functional changes in the PFC (5, 6, 30) that may promote therapeutic-like effects (10, 30). One fundamental question is how psychedelics modulate the activity of relevant circuits to drive behavioral change. Our 2-photon calcium imaging data confirmed that a subset of mPFC neurons were preferentially activated by DOI at time points when we also observed anxiolytic behavioral states. We also identified a subset of mPFC neurons that were inhibited by DOI. This is consistent with previous reports that psychedelics can either increase or decrease single-cell activity in the cortex (5, 6, 33). We used a light- and calcium-dependent transcription system scFLARE2 (24) for time-locked genetic labeling of the DOI-activated neurons, allowing us to tag DOI-activated mPFC neurons in vivo for subsequent identification. However, a limitation of existing activity-dependent tagging systems is that they cannot label inhibited neuronal populations. Thus, further study of these DOI-inhibited neurons is needed to determine their role in driving psychedelic-induced behavioral states.

snRNA-seq of scFLARE2-tagged neurons showed that DOI activates a subpopulation of cells that belong to either excitatory or inhibitory subclasses of neurons. We found only partial overlap between clusters enriched in Htr2a transcript expression and those activated by DOI. This suggests that DOI drives changes in network activity that result in the excitation of some neurons that do not express Htr2a, leading to a disconnect between 5-HT2AR expression and psychedelic-induced neuronal activity in vivo. However, differences in the overall cell counts and scFLARE2 expression across clusters could result in the missed detection of certain activated neurons. For example, the L6–2 cluster, which was a small cluster that was the most enriched in Htr2a expression, was not detected as being activated by DOI, possibly due to limitations in cluster sample size. An additional caveat of our snRNA-seq data is that because the scFLARE2 tagging requires ~24 hours for TRE-reporter gene expression, the sequencing must be performed well after the DOI has been administered. Thus, we were not able to detect acute transcriptional changes within DOI-activated mPFC neurons and were instead limited to cell-typing analysis. Future studies are needed to determine what transcriptional changes are induced across different cell-types at various timepoints after DOI injection.

Our study demonstrated that reactivation of DOI-elicited mPFC activity is sufficient to recapitulate its acute anxiolytic properties. The anxiolytic effects caused by reactivation of the DOI-tagged network requires acute 5-HT2AR activation because administration of a 5-HT2AR antagonist abolishes any behavioral effects. This suggests that the initial activation of these cells and allocation into the DOI network relies on 5-HT2ARs, although sustained receptor activation may not be necessary for the anxiolytic effects.

In this study, we did not investigate whether mPFC activity or local 5-HT2AR signaling is required for the anxiolytic effects of DOI. DOI-activated neurons in other brain regions may also be capable of driving anxiolytic behaviors upon re-activation; and there may be redundancy in the neural circuitries mediating this effect. Thus, although our study shows that these mPFC neurons serve as a critical node within a broader circuit that can mediate the anxiolytic effects of DOI, it remains to be determined what additional mechanisms activate these cells during psychedelic administration. For example, it is possible that sustained increases in activity driven by DOI induces neuronal plasticity in a specific circuit

involving the mPFC, making this network more likely to activate in the future. Through activity-dependent tagging of these DOI-responsive populations, we may be mimicking the network activation that drives these plasticity changes and induces an anxiolytic phenotype. Future studies should investigate whether there is a direct link between the mechanisms of DOI-triggered plasticity induction and the reactivation of DOI-responsive neurons.

We have shown here that it is possible to isolate the anxiolytic effects of a psychedelic drug from its hallucinogenic properties through reactivation of a DOI-tagged network. This is despite the fact that activity-dependent tagging occurred immediately after DOI injection while animals were exhibiting both reduced anxiety and hallucinogenic-like effects. This general dissociation is supported by the recent development of non-hallucinogenic psychedelic analogues that still carry therapeutic potential (20–22). Furthermore, a few studies have shown that partial 5-HT2AR antagonism eliminates the hallucinogenic effects of pychedelics in rodents, but does not fully block the beneficial behavioral and structural changes induced by psychedelics (6, 12). This raises the intriguing possibility that the anxiolytic and hallucinogenic effects of psychedelics could be mediated by separate neuronal subpopulations in the brain, or through different intracellular signaling cascades relying on distinct 5-HT2AR phosphorylation sites (44) or G protein signaling (45). We did not examine hallucinogenic-like behaviors other than the HTR, and optogenetic reactivation of DOI-tagged neurons could be driving more subtle psychedelic-related effects. Future studies may aim to identify which neural pathways and mechanisms mediate the hallucinogenic-like effects of these drugs.

Finally, although DOI's effects on anxiety- and depressive-like behaviors have been studied in animal models, it has not been investigated as a potential therapeutic for neuropsychiatric disorders in humans. Our study sheds light on cell-type specific circuit mechanisms of psychedelic action and thus advances our understanding of these highly promising drugs, a critical missing link when considering how they may affect brain function and behavior.

Supplementary Material

Refer to Web version on PubMed Central for supplementary material.

Acknowledgments:

We thank Li Ye and Will Allen for constructive feedback on the manuscript. scFLARE2 plasmids were a gift from Alice Ting (Addgene plasmid #158700, #158701, and #163036). RNA sequencing was carried out at the DNA Technologies and Expression Analysis Cores at the UC Davis Genome Center, supported by NIH Shared Instrumentation Grant 1S10OD010786-01.

Funding:

This work was supported by the following sources:

Burroughs Wellcome Fund Career Award at the Scientific Interface 1019469 (CKK)

Brain & Behavior Research Foundation Young Investigator Award 30238 (CKK)

Searle Scholars Program SSP-2022-107 (CKK)

The Kavli Foundation (CKK)

UC Davis Behavioral Health Center of Excellence Pilot Award (CKK, JM)

CIHR post-doctoral training award 202210MFE-491520-297096 (JM)

National Institutes of Health grant R25NS112130 (JMa)

National Institutes of Health grant U19NS123719 (LT)

National Institutes of Health grant U01NS120820 (LT)

Boone Family Foundation (DEO)

Camille Dreyfus Teacher-Scholar Award (DEO)

Data and materials availability:

All behavior and imaging data are available in the main text or the supplementary materials, and available from the corresponding author on request. The accession number for the single-cell RNA sequencing data reporter in this paper is GEO: GSE278644. Code supporting the current study are available at https://www.github.com/tinakimlab/MuirLin2024.

References and Notes

1. Merikangas KR et al. , Lifetime Prevalence of Mental Disorders in U.S. Adolescents: Results from the National Comorbidity Survey Replication-Adolescent Supplement (NCS-A). J Am Acad Child Psy 49, 980–989 (2010).
2. Burcusa SL, Iacono WG, Risk for Recurrence in Depression. Clin Psychol Rev 27, 959–985 (2007). [PubMed: 17448579]
3. Roth BL, Gumpper RH, Psychedelics as Transformative Therapeutics. Am J Psychiatry 180, 340–347 (2023). [PubMed: 37122272]
4. Vollenweider FX, Vollenweider-Scherpenhuyzen MF, Bäbler A, Vogel H, Hell D, Psilocybin induces schizophrenia-like psychosis in humans via a serotonin-2 agonist action. Neuroreport 9, 3897–3902 (1998). [PubMed: 9875725]
5. Ly C et al. , Psychedelics promote structural and functional neural plasticity. Cell reports 23, 3170–3182 (2018). [PubMed: 29898390]
6. Shao L-X et al. , Psilocybin induces rapid and persistent growth of dendritic spines in frontal cortex in vivo. Neuron 109, 2535–2544. e2534 (2021). [PubMed: 34228959]
7. Pei Q et al. , Serotonergic regulation of mRNA expression of Arc, an immediate early gene selectively localized at neuronal dendrites. Neuropharmacology 39, 463–470 (2000). [PubMed: 10698012]
8. Tilakaratne N, Friedman E, Genomic responses to 5-HT1a or 5-HT2a2c receptor activation is differentially regulated in four regions of rat brain. European journal of pharmacology 307, 211–217 (1996). [PubMed: 8832223]
9. Jefsen OH, Elfving B, Wegener G, Müller HK, Transcriptional regulation in the rat prefrontal cortex and hippocampus after a single administration of psilocybin. Journal of Psychopharmacology 35, 483–493 (2021). [PubMed: 33143539]
10. de la Fuente Revenga M et al. , Prolonged epigenomic and synaptic plasticity alterations following single exposure to a psychedelic in mice. Cell Rep 37, 109836 (2021). [PubMed: 34686347]
11. Pędzich BD et al. , Effects of a psychedelic 5-HT2A receptor agonist on anxiety-related behavior and fear processing in mice. Neuropsychopharmacology 47, 1304–1314 (2022). [PubMed: 35449450]
12. Hesselgrave N, Troppoli TA, Wulff AB, Cole AB, Thompson SM, Harnessing psilocybin: antidepressant-like behavioral and synaptic actions of psilocybin are independent of 5-HT2R activation in mice. Proceedings of the National Academy of Sciences 118, e2022489118 (2021).
13. Singh S et al. , Effect of psilocybin on marble burying in ICR mice: role of 5-HT1A receptors and implications for the treatment of obsessive-compulsive disorder. Translational Psychiatry 13, 164 (2023). [PubMed: 37164956]

14. Cameron LP et al. , 5-HT2ARs Mediate Therapeutic Behavioral Effects of Psychedelic Tryptamines. ACS Chem Neurosci 14, 351–358 (2023). [PubMed: 36630260]
15. Cameron LP, Benson CJ, Dunlap LE, Olson DE, Effects of NN-Dimethyltryptamine on Rat Behaviors Relevant to Anxiety and Depression. ACS Chem Neurosci 9, 1582–1590 (2018). [PubMed: 29664276]
16. Hibicke M, Landry AN, Kramer HM, Talman ZK, Nichols CD, Psychedelics, but Not Ketamine, Produce Persistent Antidepressant-like Effects in a Rodent Experimental System for the Study of Depression. ACS Chem Neurosci 11, 864–871 (2020). [PubMed: 32133835]
17. Corne S, Pickering R, Warner B, A method for assessing the effects of drugs on the central actions of 5-hydroxytryptamine. British journal of pharmacology and chemotherapy 20, 106–120 (1963). [PubMed: 14023050]
18. Halberstadt AL, Geyer MA, Characterization of the head-twitch response induced by hallucinogens in mice: detection of the behavior based on the dynamics of head movement. Psychopharmacology 227, 727–739 (2013). [PubMed: 23407781]
19. González-Maeso J et al. , Hallucinogens recruit specific cortical 5-HT2A receptor-mediated signaling pathways to affect behavior. Neuron 53, 439–452 (2007). [PubMed: 17270739]
20. Cameron LP et al. , A non-hallucinogenic psychedelic analogue with therapeutic potential. Nature 589, 474–479 (2021). [PubMed: 33299186]
21. Cao D et al. , Structure-based discovery of nonhallucinogenic psychedelic analogs. Science 375, 403–411 (2022). [PubMed: 35084960]
22. Kaplan AL et al. , Bespoke library docking for 5-HT(2A) receptor agonists with antidepressant activity. Nature 610, 582–591 (2022). [PubMed: 36171289]
23. Kim CK et al. , A Molecular calcium integrator reveals a striatal cell type driving aversion. Cell 183, 2003–2019. e2016 (2020). [PubMed: 33308478]
24. Sanchez MI, Nguyen Q-A, Wang W, Soltesz I, Ting AY, Transcriptional readout of neuronal activity via an engineered Ca2+-activated protease. Proceedings of the National Academy of Sciences 117, 33186–33196 (2020).
25. Odland AU, Kristensen JL, Andreasen JT, Investigating the role of 5-HT2A and 5-HT2C receptor activation in the effects of psilocybin, DOI, and citalopram on marble burying in mice. Behav Brain Res 401, 113093 (2021). [PubMed: 33359368]
26. Odland AU, Jessen L, Kristensen JL, Fitzpatrick CM, Andreasen JT, The 5-hydroxytryptamine 2A receptor agonists DOI and 25CN-NBOH decrease marble burying and reverse 8-OH-DPAT-induced deficit in spontaneous alternation. Neuropharmacology 183, 107838 (2021). [PubMed: 31693871]
27. Dhonnchadha B. d. Á. N., Bourin M, Hascoët M, Anxiolytic-like effects of 5-HT2 ligands on three mouse models of anxiety. Behavioural brain research 140, 203–214 (2003). [PubMed: 12644293]
28. de la Fuente Revenga M et al. , Fully automated head-twitch detection system for the study of 5-HT(2A) receptor pharmacology in vivo. Sci Rep 9, 14247 (2019). [PubMed: 31582824]
29. Dong C et al. , Psychedelic-inspired drug discovery using an engineered biosensor. Cell 184, 2779–2792. e2718 (2021). [PubMed: 33915107]
30. Vargas MV et al. , Psychedelics promote neuroplasticity through the activation of intracellular 5 HT2A receptors. Science 379, 700–706 (2023). [PubMed: 36795823]
31. Riga D et al. , Optogenetic dissection of medial prefrontal cortex circuitry. Frontiers in systems neuroscience 8, 230 (2014). [PubMed: 25538574]
32. Chen T-W et al. , Ultrasensitive fluorescent proteins for imaging neuronal activity. Nature 499, 295 (2013). [PubMed: 23868258]
33. Wood J, Kim Y, Moghaddam B, Disruption of prefrontal cortex large scale neuronal activity by different classes of psychotomimetic drugs. Journal of Neuroscience 32, 3022–3031 (2012). [PubMed: 22378875]
34. Brys I et al. , 5-HT2AR and NMDAR psychedelics induce similar hyper-synchronous states in the rat cognitive-limbic cortex-basal ganglia system. Communications Biology 6, 737 (2023). [PubMed: 37495733]

35. Michaiel AM, Parker PR, Niell CM, A hallucinogenic serotonin-2A receptor agonist reduces visual response gain and alters temporal dynamics in mouse V1. Cell reports 26, 3475–3483. e3474 (2019). [PubMed: 30917304]
36. Lui JH et al. , Differential encoding in prefrontal cortex projection neuron classes across cognitive tasks. Cell 184, 489–506. e426 (2021). [PubMed: 33338423]
37. Bhattacherjee A et al. , Cell type-specific transcriptional programs in mouse prefrontal cortex during adolescence and addiction. Nature communications 10, 4169 (2019).
38. Fantegrossi WE et al. , Interaction of 5-HT2A and 5-HT2C receptors in R (−)-2, 5-dimethoxy-4-iodoamphetamine-elicited head twitch behavior in mice. Journal of Pharmacology and Experimental Therapeutics 335, 728–734 (2010). [PubMed: 20858706]
39. Canal CE et al. , The serotonin 2C receptor potently modulates the head-twitch response in mice induced by a phenethylamine hallucinogen. Psychopharmacology 209, 163–174 (2010). [PubMed: 20165943]
40. Kim CK et al. , Simultaneous fast measurement of circuit dynamics at multiple sites across the mammalian brain. Nature methods 13, 325–328 (2016). [PubMed: 26878381]
41. Onaivi ES, Bishop-Robinson C, Darmani NA, Sanders-Bush E, Behavioral effects of (±)-1-(2, 5-dimethoxy-4-iodophenyl)-2-aminopropane,(DOI) in the elevated plus-maze test. Life sciences 57, 2455–2466 (1995). [PubMed: 8847967]
42. Goodwin GM et al. , Single-Dose Psilocybin for a Treatment-Resistant Episode of Major Depression. N Engl J Med 387, 1637–1648 (2022). [PubMed: 36322843]
43. Raison CL et al. , Single-Dose Psilocybin Treatment for Major Depressive Disorder: A Randomized Clinical Trial. JAMA 330, 843–853 (2023). [PubMed: 37651119]
44. Karaki S et al. , Quantitative phosphoproteomics unravels biased phosphorylation of serotonin 2A receptor at Ser280 by hallucinogenic versus nonhallucinogenic agonists. Molecular & Cellular Proteomics 13, 1273–1285 (2014). [PubMed: 24637012]
45. Liu X et al. , Gs signaling pathway distinguishes hallucinogenic and nonhallucinogenic 5-HT2AR agonists induced head twitch response in mice. Biochemical and Biophysical Research Communications 598, 20–25 (2022). [PubMed: 35149433]
46. Konermann S et al. , Optical control of mammalian endogenous transcription and epigenetic states. Nature 500, 472–476 (2013). [PubMed: 23877069]
47. Pachitariu M et al. , Suite2p: beyond 10,000 neurons with standard two-photon microscopy. BioRxiv, 061507 (2016).
48. Hodneland E, Kögel T, Frei DM, Gerdes H-H, Lundervold A, CellSegm-a MATLAB toolbox for high-throughput 3D cell segmentation. Source code for biology and medicine 8, 16 (2013). [PubMed: 23938087]
49. Wolf FA, Angerer P, Theis FJ, SCANPY: large-scale single-cell gene expression data analysis. Genome biology 19, 15 (2018). [PubMed: 29409532]
50. Yao Z et al. , A taxonomy of transcriptomic cell types across the isocortex and hippocampal formation. Cell 184, 3222–3241 e3226 (2021). [PubMed: 34004146]

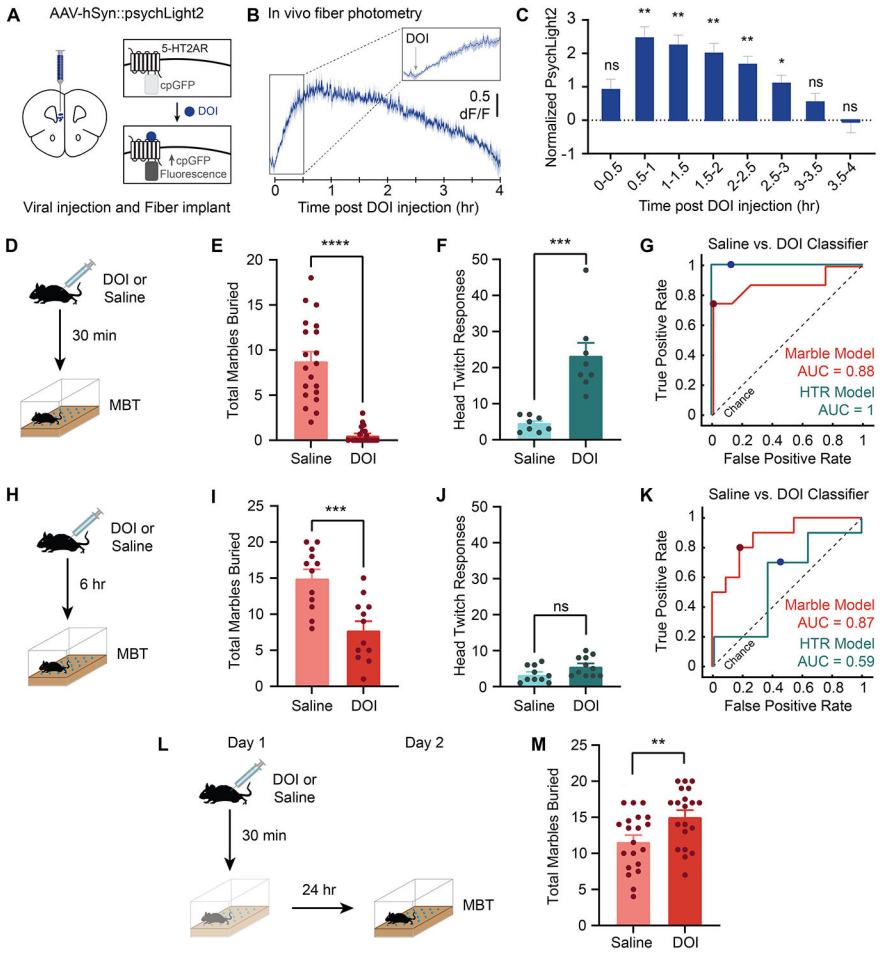

Fig. 1. DOI can reduce anxiety-like behaviors beyond its hallucinogenic effects.

(**A**) Schematic of psychLight2 fluorescent sensor and AAV-hSyn::psychLight2 injection location in the mPFC of mice. (**B**) PsychLight2 fluorescence signal measured over the course of 4 hours after a 6 mg/kg DOI injection (n = 6 mice). (**C**) Mean binned psychLight2 fluorescence signal from panel (B), normalized by subtracting the baseline signal before DOI injection. (**D**) Schematic of MBT behavioral paradigm performed 30 minutes after DOI injection. (**E**) Total number of marbles buried during the MBT for mice injected with either saline or DOI (n = 20 mice per group). (**F**) Number of HTRs during the first 10 minutes of the MBT (n = 8 mice per group). (**G**) ROC curves for classifiers predicting saline versus DOI treatment, modeled using either the number of marbles buried (“Marble Model”) or the number of head twitches (“HTR Model”) (n = 8 mice per classifier, 8-fold cross-validation). Solid dots represent the model operating point. (**H**) Schematic of MBT behavioral paradigm performed 6 hours after DOI injection. (**I**) Total number of marbles buried during the MBT for mice injected with either saline or DOI (n = 12 mice per group). (**J**) Number of head twitch responses during the first 10 minutes of the MBT (n = 10 to 11 mice per group). (**K**) ROC curves for classifiers predicting saline versus DOI treatment, as in panel (G) (n = 10 to 11 mice per classifier). (**L**) Schematic of MBT behavioral paradigm performed in mice from panels (D)-(G), but 24 hours later. (**M**) Total number of marbles buried during the MBT for mice injected with either saline or DOI (n = 20 mice per group). Data are plotted as mean ±

SEM. *P* values were calculated using a One-way repeated measures ANOVA with Dunnett's multiple comparisons test in panel (C), and an unpaired Student's *t*-test in panels (E), (F), (I), (J), and (M). $*P < 0.05$, $**P < 0.01$, $***P < 0.001$, $****P < 0.0001$; ns, not significant.

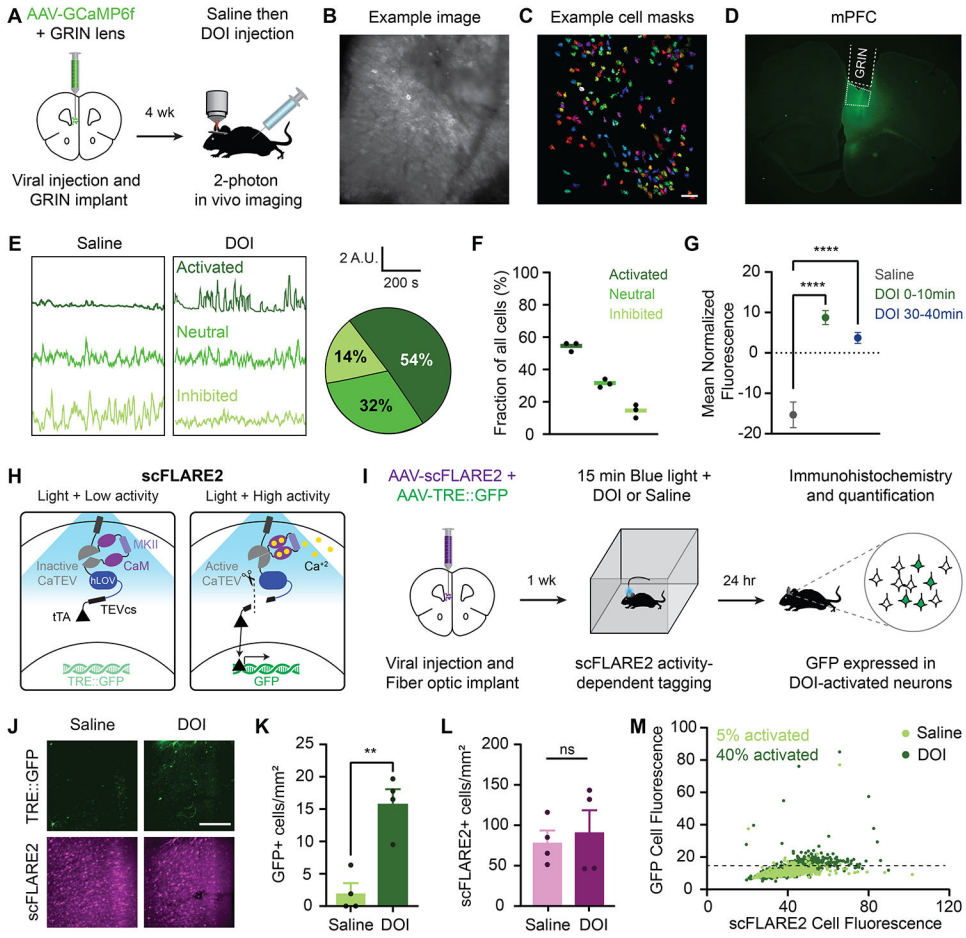

Fig. 2. Recording and tagging DOI-activated neuronal ensembles in vivo.

(**A**) Experimental timeline. Mice were injected with AAV-CaMK2a::GCaMP6f in mPFC, and a GRIN lens was implanted above to allow for single-cell 2-photon calcium imaging. (**B**) Example mean GCaMP6f image and (**C**) cell masks from a single FOV identified using Suite2P. Scale bar, 140 μm. (**D**) Histology image showing viral expression and GRIN lens placement above mPFC. (**E**) Representative calcium fluorescence traces from DOI-activated, DOI-inhibited, and neutral (unchanged) neurons (see “Materials and Methods” for classification details). Pie chart shows percentage of neurons belonging to each group (n = 361 neurons pooled from 3 mice). (**F**) Data from pie chart in panel (E), averaged for each biological replicate (n = 3 mice). (**G**) Mean normalized fluorescence of DOI-activated cells during the saline period, 0–10 min after DOI injection, and 30–40 min after DOI injection (n = 2 mice). (**H**) Schematic of scFLARE2. The presence of both light and calcium triggers the release of the transcription factor, tTA, which translocates to the nucleus to drive the expression of the reporter gene, TRE::GFP. (**I**) Experimental timeline. Mice were injected with AAV-hSyn::scFLARE2 and AAV-TRE::GFP in mPFC, and a fiber-optic cannula was implanted above. Immediately after injection with DOI or saline, blue light was delivered to the mPFC to allow for scFLARE2 tagging and activity-dependent GFP expression. (**J**) Representative fluorescence images of scFLARE2 and GFP expression. Scale bar, 130 μm. (**K**) Quantification of the number of GFP+ cells/mm^2 in mice treated with either saline or

DOI (n = 4 slices from 2 mice per group). (**L**) Quantification of the number of scFLARE2+ cells/mm^2 in mice treated with either saline or DOI (n = 4 slices per group). (**M**) GFP fluorescence as a function of scFLARE2 fluorescence for all scFLARE2+ cells. Dashed line indicates the GFP activation threshold, which is defined as the 95th percentile of GFP cell fluorescence in saline mice. Data are plotted as mean ± SEM. P values were calculated using a One-way repeated measures ANOVA with Tukey's multiple comparisons test in panel (G), and an unpaired Student's t-test in panels (K) and (L). **P<0.01, ****P < 0.0001; ns, not significant.

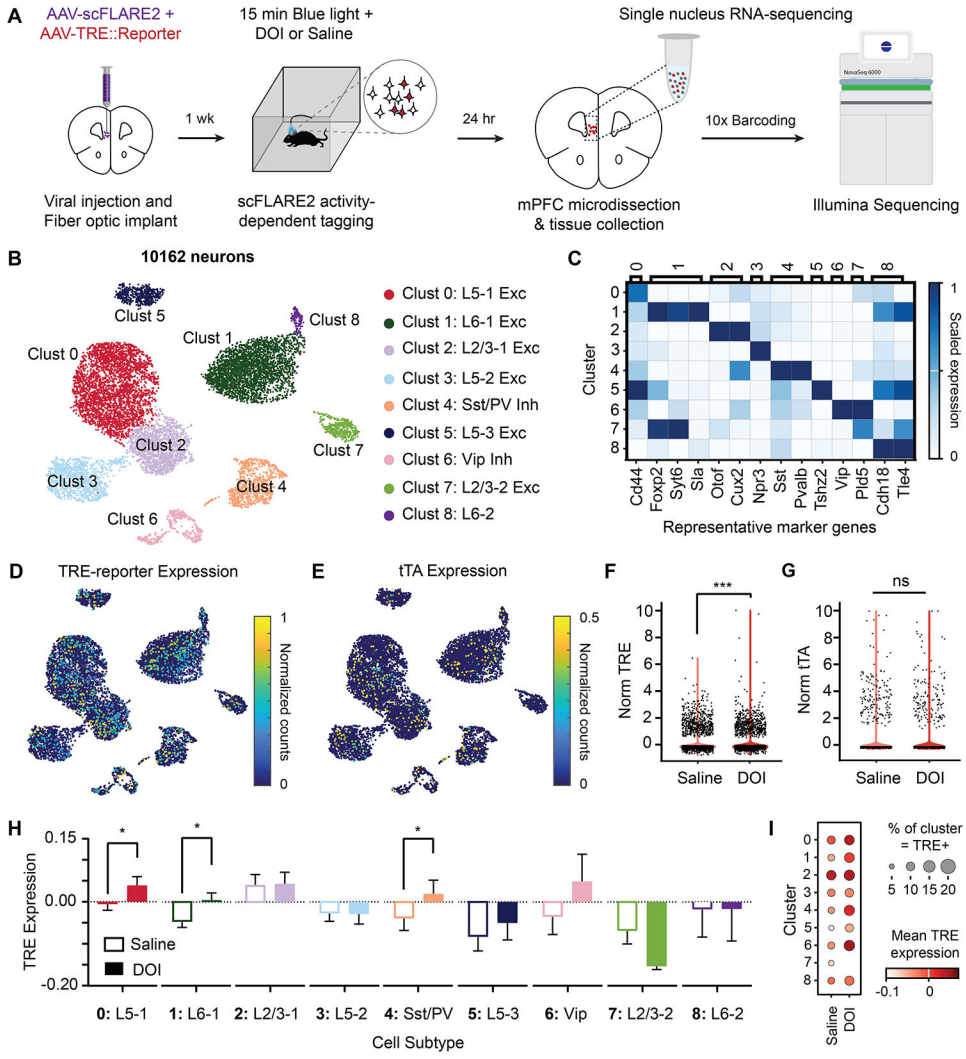

Fig. 3. snRNA-seq of scFLARE2-tagged neurons reveals DOI-induced network activation.

(**A**) Experimental timeline. Mice were injected with AAV-hSyn::scFLARE2 and AAV-TRE::mCherry-p2a-bReaChES in the mPFC. 24 hours after scFLARE2 tagging, the mPFC was micro-dissected and dissociated into single nuclei. Nuclei were barcoded using a 3' 10x library kit followed by Illumina next-gen sequencing. (**B**) UMAP visualization of individual nuclei corresponding to different neuronal cell-types. (**C**) Heatmap showing the expression of representative cell-type marker genes reported from prior mouse mPFC snRNA-seq datasets. (**D-E**) UMAP visualization of log1p normalized TRE-reporter and tTA expression in all nuclei across clusters. (**F-G**) Average log1p normalized TRE-reporter and tTA expression in all nuclei between saline and DOI treated animals. (**H**) Average unit variance scaled, log1p normalized TRE-reporter gene expression across nuclei within each cluster for saline- and DOI-treated animals (**I**) Dot plot representing the fraction of nuclei within each cluster that are mCherry+ (unit variance scaled, log1p normalized count > 0). *P* values in panels (F) and (G) were calculated using an unpaired Student's *t*-test; ****P* < 0.001, ns, not significant. Data in panel (H) are plotted as mean ± SEM, and FDR values were calculated following a 1-sided permutation test with 10,000 shuffles; **FDR* < 0.05.

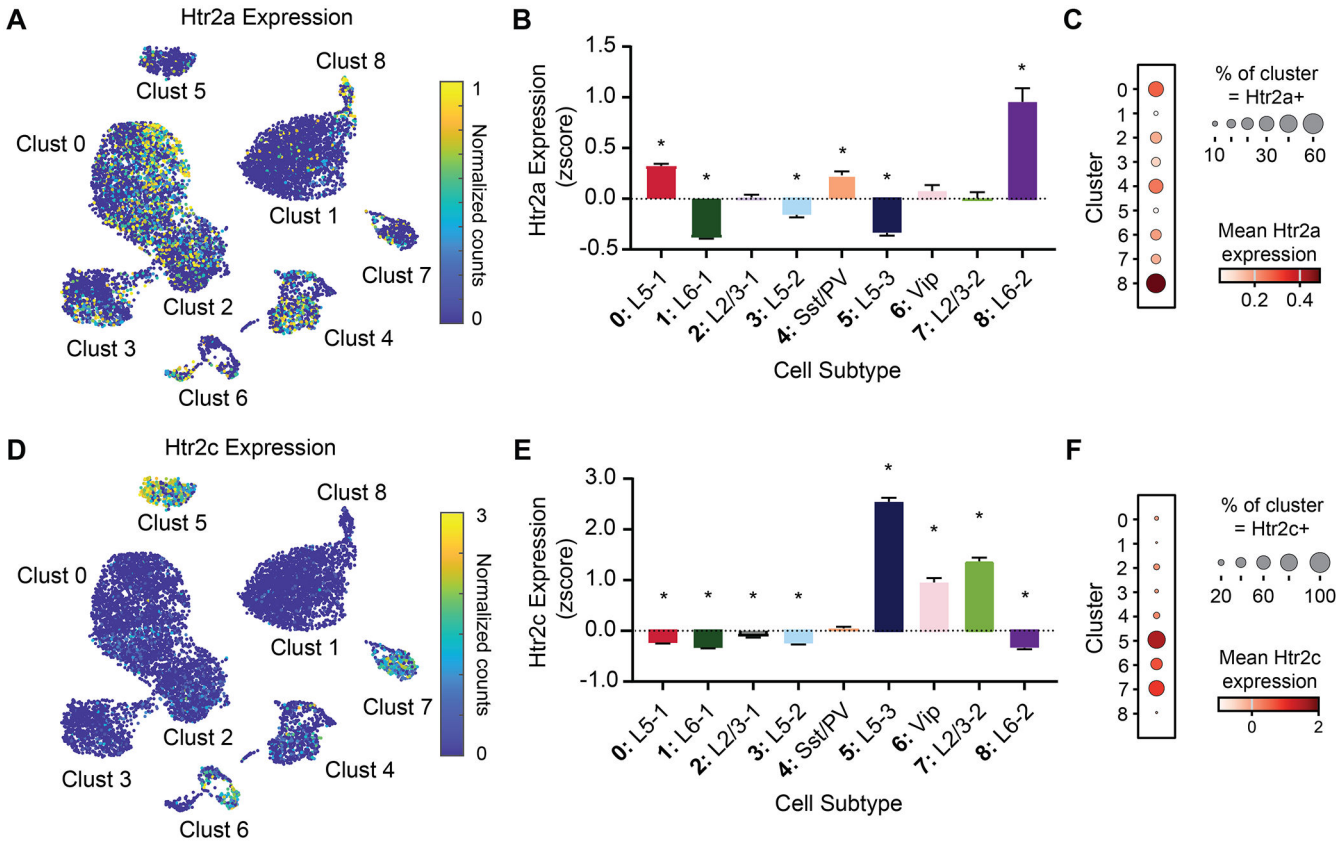

Fig. 4. 5-HT2A/C receptor expression in scFLARE2-tagged neuronal clusters.

(**A**) UMAP visualization of log1p normalized Htr2a expression in all nuclei across clusters. (**B**) Average Z-scored, log1p normalized Htr2a expression of all nuclei within each cluster. (**C**) Dot plot representing the fraction of nuclei within each cluster that are Htr2a+ (log1p normalized count > 0). (**D-F**) Same as panels (A-C), except for Htr2c. Data are plotted as mean ± SEM. *P* values were calculated using a Wilcoxon Rank-sum test with Bonferroni correction testing in panel (B,E). *adjusted $P < 0.0001$.

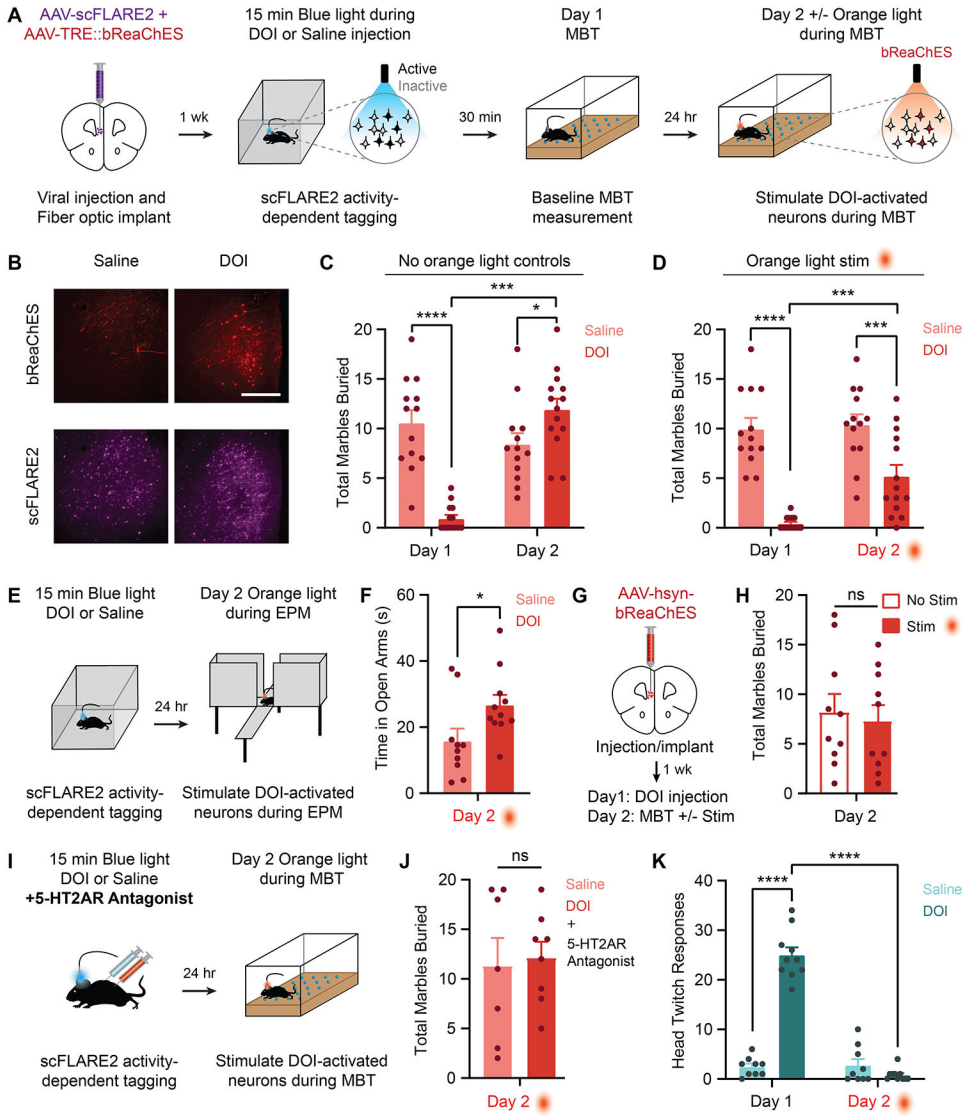

Fig. 5. Reactivation of DOI-tagged neurons reduces anxiety-like behaviors without hallucinogenic side-effects.

(**A**) Experimental timeline. Mice were injected with AAV-hSyn::scFLARE2 and AAV-TRE::mCherry-p2a-bReaChES in mPFC. (**B**) Representative fluorescence images of scFLARE2 and mCherry-p2a-bReaChES expression. Scale bar, 130 μm. (**C**) Total number of marbles buried by control mice undergoing saline- or DOI-tagging, but not receiving orange light stimulation on day 2 (n = 13 to 14 mice per group). (**D**) Total number of marbles buried by mice receiving orange light stimulation of saline- or DOI-tagged neurons on day 2 (n = 13 to 14 mice per group). (**E**) Experimental timeline. Mice were prepared as in panel (A) and given blue light during DOI or saline injection. 24 hours later, they underwent an EPM assay. (**F**) Time spent in the open arms of the EPM by mice receiving orange light stimulation of saline- or DOI-tagged mPFC neurons on day 2 (n = 10 to 11 mice per group). (**G**) Mice were injected with AAV-hSyn::mCherry-p2a-bReaChES in the mPFC for non-specific stimulation and underwent an MBT assay on day 2. (**H**) Total number of marbles buried by mice receiving no light or orange light stimulation on day 2 (n = 10 mice

per group). (**I**) Experimental timeline. Mice were prepared as in panel (A) but received a 5-HT2AR antagonist with either DOI or saline injection. 24 hours after tagging, mice were run through the MBT with orange light stimulation. (**J**) Total number of marbles buried by mice receiving orange light stimulation on day 2 (n = 7 to 8 mice per group). (**K**) Number of HTRs during the first 10 minutes of the MBT on day 1 after saline or DOI injection, or on day 2 during orange light stimulation of saline- or DOI-tagged mPFC neurons (n = 9 to 10 mice per group). Data are plotted as mean ± SEM. P values were calculated using a Two-way ANOVA with Tukey's multiple comparisons test in panels (C), (D), and (K), and an unpaired Student's t-test in panels (F), (H), and (J). *P < 0.05, ***P < 0.001, ****P < 0.0001; ns, not significant.